

Polarized fermions in the unitarity limit

Gautam Rupak* and Thomas Schäfer†

Department of Physics, North Carolina State University, Raleigh, NC 27695

Andrei Kryjevski‡

Nuclear Theory Center, Indiana University, Bloomington, IN 47408

We consider a polarized Fermi gas in the unitarity limit. Results are calculated analytically up to next-to-leading order in an expansion about $d = 4$ spatial dimensions. We find a first order transition from superfluid to normal phase. The critical chemical potential asymmetry for this phase transition is $\delta\mu_c = \frac{2\mu}{\varepsilon}(1 - 0.467\varepsilon)$, where $\varepsilon = 4 - d$ is the expansion parameter and μ is the average chemical potential of the two fermion species. Stability of the superfluid phase in the presence of supercurrents is also studied.

I. INTRODUCTION

Recently, there has been a lot of interest in the quantum phase transition between a paired fermion superfluid and a normal Fermi liquid that occurs as the difference in the chemical potentials of the up and down spins is increased. This transition is well understood in the strong coupling Bose-Einstein condensation (BEC) and weak coupling Bardeen-Cooper-Schrieffer (BCS) limits, but the nature of the phase diagram near the BEC/BCS crossover remains to be elucidated. The BEC/BCS crossover is characterized by a divergent atom-atom scattering length. Over the last year, first results from experiments with polarized atomic systems near a Feshbach resonance have appeared [1, 2, 3].

Theoretically the regime of large scattering lengths is difficult since the standard perturbative methods are not applicable. Based on an observation by Nussinov and Nussinov [4], Nishida and Son [5] proposed an analytic method for calculating thermodynamic properties as an expansion around $d = 4$ spatial dimensions. One starts by performing the calculation in arbitrary $d = 4 - \varepsilon$ space dimensions and develops a perturbative expansion in ε . In this formalism, the Cooper pair energy χ_0 is considered $\mathcal{O}(1)$ and the chemical potential $\mu \sim \mathcal{O}(\varepsilon)$. A next-to-leading order calculation [5] of the superfluid gap and the equation of state agrees well with fixed node Green Function Monte Carlo [6, 7, 8, 9] and Euclidean Path Integral [10, 11] calculations. Somewhat smaller values of the energy per particle and the energy gap were obtained in the canonical Path Integral Monte Carlo calculation [12]. For a polarized system with chemical potential difference $\delta\mu$, we expect the superfluid phase to become unstable when the asymmetry is on the order of the gap in the symmetric system $\delta\mu \sim \chi_0$ [13, 14, 15]. Thus we will consider a situation where $\mu \sim \varepsilon \ll \chi_0 \sim 1 \sim \delta\mu$.

At unitarity, the fermionic system at non-zero density is de-

scribed by the Lagrangian density [5]

$$\mathcal{L} = \Psi^\dagger \left[i\partial_0 + \delta\mu + \sigma_3 \frac{\nabla^2}{2m} \right] \Psi + \mu \Psi^\dagger \sigma_3 \Psi + \left(\Psi^\dagger \sigma_+ \Psi \phi + h.c. \right), \quad (1)$$

with an asymmetry parameterized by $\delta\mu$. $\Psi = (\psi_\uparrow, \psi_\downarrow)^T$ is a two-component Nambu-Gor'kov field. σ_i 's are Pauli matrices acting on Nambu-Gor'kov space and $\sigma_\pm = (\sigma_1 \pm i\sigma_2)/2$. Effects from large but finite 2-body scattering length could also be studied. Calculations in the few-body systems agree well with numerical results [16].

In the superfluid state $\langle \phi \rangle = \chi = \chi^\dagger$. Expanding about χ ($\phi = \chi + g\phi$), the Lagrangian density is written in terms of the free piece \mathcal{L}_0 and interacting piece \mathcal{L}_I :

$$\begin{aligned} \mathcal{L}_0 &= \Psi^\dagger \left[i\partial_0 + \delta\mu + \sigma_3 \frac{\nabla^2}{2m} + \chi(\sigma_+ + \sigma_-) \right] \Psi \\ &\quad + \phi^\dagger \left(i\partial_0 + \frac{\nabla^2}{4m} \right) \phi, \\ \mathcal{L}_I &= g \left(\Psi^\dagger \sigma_+ \Psi \phi + h.c. \right) + \mu \Psi^\dagger \sigma_3 \Psi - \phi^\dagger \left(i\partial_0 + \frac{\nabla^2}{4m} \right) \phi, \\ g &= \frac{\sqrt{8\pi^2\varepsilon}}{m} \left(\frac{m\chi}{2\pi} \right)^{\varepsilon/4}. \end{aligned} \quad (2)$$

The fermion Ψ and boson ϕ propagators are

$$\begin{aligned} G(p_0, \mathbf{p}) &= \frac{i}{(p_0 + \delta\mu)^2 - E_p} \begin{bmatrix} p_0 + \delta\mu + \omega_p & -\chi \\ -\chi & p_0 + \delta\mu - \omega_p \end{bmatrix}, \\ D(p_0, \mathbf{p}) &= \frac{i}{p_0 - \frac{p^2}{4m}}, \end{aligned} \quad (3)$$

where $\omega_p = p^2/(2m)$ and $E_p = \sqrt{\omega_p^2 + \chi^2}$. The “ i -delta” prescription for the interacting theory is $p_0 \rightarrow p_0(1 + i\delta)$.

II. THERMODYNAMIC POTENTIAL

The calculation of the thermodynamic potential with non-zero $\delta\mu$ is very similar to the $\delta\mu = 0$ calculation of Ref. [5].

*Electronic address: grupak@u.washington.edu

†Electronic address: thomas.schaefer@ncsu.edu

‡Electronic address: akryjevs@indiana.edu

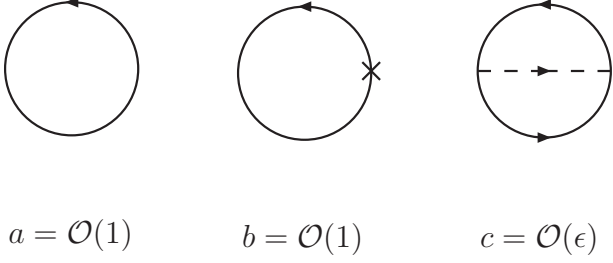


FIG. 1: Leading order contributions to the thermodynamic potential in the ϵ -expansion. The solid lines are fermions, and the dashed lines are bosons. The “x” represents insertion of $\mu\sigma_3$.

The main difference is that the $\delta\mu$ dependent pieces get contribution from momenta p in a window $p \lesssim \sqrt{2m\delta\mu}$ [17, 18]. In particular, the first 1-loop diagram in Fig. 1 gives a $\mathcal{O}(1)$ $\delta\mu$ contribution to the effective potential. The second diagram is also $\mathcal{O}(1)$. However, the $\delta\mu$ contribution is $\mathcal{O}(\epsilon)$ since the diagram is proportional to an insertion of $\mu \sim \epsilon$ and there is no $1/\epsilon$ enhancement from the finite volume loop-integral for momenta $p \lesssim \sqrt{2m\delta\mu}$. The 2-loop diagram is $\mathcal{O}(\epsilon)$ due to the factors of g^2 from the vertices.

The first 1-loop diagram from Fig. 1 gives:

$$\frac{a}{m^{d+1}} = \int \frac{d^d p_0}{2\pi} \frac{d^d p}{(2\pi)^d} \frac{\log[(p_0 + \delta\mu)^2 - E_p^2]}{m^{d+1}}. \quad (4)$$

We divide the free energy by factors of $m^{d+1} = m^{5-\epsilon}$ to look at dimensionless quantities for convenience. Without the loss of any generality, we choose $\delta\mu \geq 0$. Then,

$$\begin{aligned} \frac{a}{m^{d+1}} &= i \int \frac{d^d p}{(2\pi)^d} \frac{E_p}{m^{d+1}} + i \int_{p \leq p_0} \frac{d^d p}{(2\pi)^d} \frac{\delta\mu - E_p}{m^{d+1}} \Theta(\delta\mu - \chi) \\ &\approx -i \frac{2\chi^3 - (\delta\mu - \chi)^2 (\delta\mu + 2\chi) \Theta(\delta\mu - \chi)}{24\pi^2 m^3} + \mathcal{O}(\epsilon), \end{aligned} \quad (5)$$

with $p_0^2 = 2m\sqrt{\delta\mu^2 - \chi^2}$. The contribution from the second 1-loop diagram in Fig. 1 gives

$$\begin{aligned} \frac{b}{m^{d+1}} &= -i \int \frac{d^d p_0}{2\pi} \frac{d^d p}{(2\pi)^d} \frac{G_{11}(p_0, \mathbf{p}) - G_{22}(p_0, \mathbf{p})}{m^{d+1}} \\ &= -i \frac{\mu}{m^{d+1}} \left[\int \frac{d^d p}{(2\pi)^d} \frac{\omega_{\mathbf{p}}}{E_p} - \int_{p \leq p_0} \frac{d^d p}{(2\pi)^d} \frac{\omega_{\mathbf{p}}}{E_p} \Theta(\delta\mu - \chi) \right] \\ &\approx i \frac{\chi^2 \mu}{4\pi^2 m^3 \epsilon} + \mathcal{O}(\epsilon), \end{aligned} \quad (6)$$

where $\mu \sim \mathcal{O}(\epsilon)$. Thus the leading order effective potential is

$$\begin{aligned} \frac{V_0(\chi; \delta\mu)}{m^{d+1}} &= i \frac{a+b}{m^{d+1}} \approx - \frac{(\delta\mu - \chi)^2 (\delta\mu + 2\chi)}{24\pi^2 m^3} \Theta(\delta\mu - \chi) \\ &\quad + \frac{\chi^2 (\chi - 3\mu/\epsilon)}{12\pi^2 m^3}. \end{aligned} \quad (7)$$

In Fig. 2, we plot the leading order effective potential V_0 as a function of χ for various values of $\delta\mu$. For $\delta\mu < 2\mu/\epsilon$, the

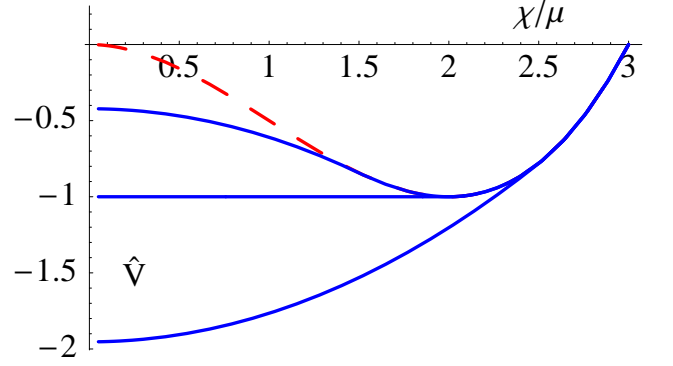


FIG. 2: The leading order dimensionless effective potential $\hat{V} = 3 \frac{V_0}{\mu} \left(\frac{\pi}{m\mu} \right)^2$ as a function of χ/μ for increasing values of $\delta\mu$. The dashed curve shows the result for $\delta\mu = 0$, and the solid curves are for non-zero $\delta\mu$. For $\delta\mu < 2\mu$, superfluid phase has lower energy. For $\delta\mu > 2\mu$, the normal phase is preferred and for $\delta\mu = 2\mu = \chi_0$ a unique phase equilibrium characterized by the second curve from bottom exists.

ground state is a superfluid and the potential V_0 is minimized by $\chi_0 = 2\mu/\epsilon$. At $\delta\mu = 2\mu/\epsilon$, $V_0(\chi) = V_0(\chi_0) - m^2 \mu^3 / (3\pi^2 \epsilon^3)$ for all $\chi \leq \delta\mu_c = 2\mu/\epsilon$. This is qualitatively different from weak coupling BCS results where the normal and BCS phases are separated by a potential barrier. At leading order in the ϵ expansion the superfluid phase is stable all the way up to $\delta\mu \leq \chi_0$, compared to the weak coupling BCS result $\delta\mu \leq \chi_0/\sqrt{2}$. In addition to that, there is no unstable gapless Sarma phase [13, 17, 18, 19] for any value of $\delta\mu$, while BCS calculations predict the presence of a Sarma phase for $\chi_0/2 \leq \delta\mu \leq \chi_0$.

To understand the nature of the transition from superfluid phase to normal phase better, it is necessary to consider the next-to-leading order corrections. *A priori* it seems unlikely that the “flatness” of the potential for $\chi \leq \delta\mu$ at the critical $\delta\mu_c$ will be maintained at higher orders in the expansion. The calculation can be simplified by expanding $\delta\mu$ around the leading order value at the critical point, $\delta\mu = 2\mu/\epsilon + \epsilon\delta\mu'$.

The first 1-loop diagram gives:

$$\begin{aligned} a &= i \int \frac{d^d p}{(2\pi)^d} E_p + i \int \frac{d^d p}{(2\pi)^d} \left(\frac{2\mu}{\epsilon} - E_p \right) \Theta\left(\frac{2\mu}{\epsilon} - E_p \right) \\ &\quad + i\epsilon\delta\mu' \int \frac{d^d p}{(2\pi)^d} \Theta(2\mu/\epsilon - E_p) \\ \frac{a}{m^{d+1}} &\approx -i \frac{\chi^3}{12\pi^2 m^3} \left[1 + \frac{7 - 3\gamma_E + 3 \log(m\pi/\chi)}{6} \epsilon \right] \\ &\quad + i\epsilon\delta\mu' \frac{4\mu^2/\epsilon^2 - \chi^2}{8\pi^2 m^3} \Theta(2\mu/\epsilon - \chi) \\ &\quad + i \frac{1}{m^{d+1}} \int \frac{d^d p}{(2\pi)^d} \left(\frac{2\mu}{\epsilon} - E_p \right) \Theta(2\mu/\epsilon - E_p) + \mathcal{O}(\epsilon^2). \end{aligned} \quad (8)$$

$\gamma_E \approx 0.57722$ is the Euler-Mascheroni constant. The factors of m^d are understood to be expanded to the appropriate order in $\epsilon = 4 - d$. The $\mathcal{O}(1)$ contribution from the last term was

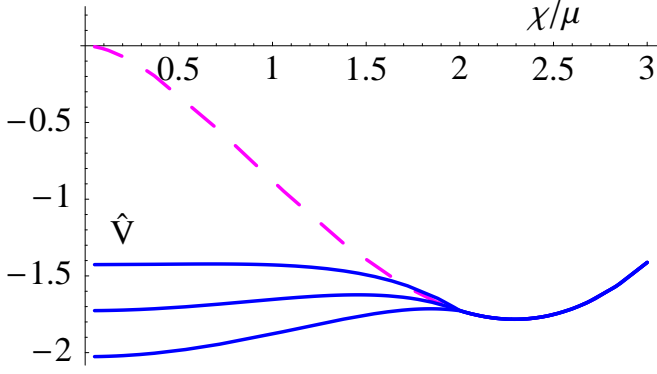


FIG. 3: The next-to-leading order dimensionless effective potential $\hat{V} = 3\frac{V_1}{\mu} \left(\frac{\pi}{m\mu}\right)^{d/2}$ as a function of χ/μ . Factors of $(m\mu)^{d/2}$ are understood to be expanded to the appropriate order in $\varepsilon = 4 - d$. The dashed curve shows the result for $\delta\mu = 0$, and the solid curves are for three different values of $\delta\mu$ near $2\mu/\varepsilon$.

already calculated in Eq. (5). The $\mathcal{O}(\varepsilon)$ can be calculated analytically but the expression is not very illuminating and we will not write it explicitly.

At next-to-leading order the contribution from the second 1-loop diagram in Fig. 1 is

$$\begin{aligned} \frac{b}{m^{d+1}} \approx & i \frac{\mu \chi^2}{4\pi^2 m^3 \varepsilon} \left[1 + \frac{1 - 2\gamma_E + 2 \log(4m\pi/\chi)}{4} \varepsilon \right] \\ & + i \frac{\mu}{8\pi^2 m^3} \left(\frac{2\mu}{\varepsilon} \sqrt{\frac{4\mu^2}{\varepsilon^2} - \chi^2} - \chi^2 \sinh^{-1} \sqrt{\frac{4\mu^2}{\chi^2 \varepsilon^2} - 1} \right) \\ & \Theta(2\mu/\varepsilon - \chi), \end{aligned} \quad (9)$$

where we have used $\delta\mu \approx 2\mu/\varepsilon + \mathcal{O}(\varepsilon)$. The 2-loop contribution from Fig. 1 is

$$\begin{aligned} \frac{c}{m^{d+1}} = & g^2 \int \frac{d^{d+1}p}{(2\pi)^{d+1}} \frac{d^{d+1}q}{(2\pi)^{d+1}} \frac{G_{11}(p)G_{22}(q)D(p-q)}{m^{d+1}} \\ \approx & i\varepsilon \frac{\chi^3}{4\pi^2 m^3} [\hat{C} - \hat{D} - \hat{E}] + \mathcal{O}(\varepsilon^2), \end{aligned} \quad (10)$$

where

$$\begin{aligned} \hat{C} = & \int_0^\infty dx \int_0^\infty dy \frac{[f(x)-x][f(y)-y]}{f(x)f(y)} \\ & \times \left[j(x,y) - \sqrt{j(x,y)^2 - xy} \right] \end{aligned} \quad (11)$$

is the $\delta\mu$ independent piece and

$$\begin{aligned} \hat{D} = & \int_0^\infty dx \int_0^\lambda dy \frac{[f(x)-x][f(y)-y]}{f(x)f(y)} \\ & \times \left[j(x,y) - \sqrt{j(x,y)^2 - xy} \right] \Theta(\delta\mu - \chi), \\ \hat{E} = & \int_0^\lambda dx \int_\lambda^\infty dy \frac{[f(x)+x][f(y)-y]}{f(x)f(y)} \\ & \times \left[k(x,y) + \sqrt{k(x,y)^2 - xy} \right] \Theta(\delta\mu - \chi), \end{aligned} \quad (12)$$

are the $\delta\mu$ corrections. We have defined the functions

$$\begin{aligned} j(x,y) &= f(x) + f(y) + (x+y)/2, \\ k(x,y) &= f(x) - f(y) - (x+y)/2, \\ f(x) &= \sqrt{x^2 + 1}, \quad \lambda = \sqrt{\delta\mu^2/\chi^2 - 1}. \end{aligned} \quad (13)$$

Numerical evaluation gives $\hat{C} \approx 0.14424$. The contribution from the 2-loop diagram is $\mathcal{O}(\varepsilon)$. Therefore we can use $\delta\mu = 2\mu/\varepsilon$ in the integrals \hat{D} , \hat{E} at this order of the calculation.

At next-to-leading order in the ε -expansion, the effective potential is

$$V_1 = i(a + b + c), \quad (14)$$

where we use $\delta\mu = 2\mu/\varepsilon + \varepsilon\delta\mu' + \mathcal{O}(\varepsilon^2)$. Results are plotted in Fig. 3 for various values of $\delta\mu'$. The next-to-leading order result is qualitatively similar to weak coupling BCS theory with a stable and unstable superfluid phase. The stable superfluid phase is at [5]

$$\chi_0 \approx \frac{2\mu}{\varepsilon} [1 + (3\hat{C} - 1 + \log 2)\varepsilon]. \quad (15)$$

The critical chemical potential $\delta\mu_c$ when the normal and stable superfluid phase are in equilibrium can be determined analytically by equating the corresponding pressures:

$$V_1(\chi = 0; \delta\mu_c) = V_1(\chi_0; \delta\mu_c). \quad (16)$$

This is further simplified because $V_1(\chi_0; \delta\mu_c) = V_1(\chi_0, 0)$. We find

$$\begin{aligned} \delta\mu_c \approx & \frac{2\mu}{\varepsilon} \left[1 + \frac{12\hat{C} - 8 + 5 \log 2}{6} \varepsilon \right] \\ \approx & \frac{2\mu}{\varepsilon} (1 - 0.4672\varepsilon). \end{aligned} \quad (17)$$

III. FERMION DISPERSION RELATION

The fermion dispersion relation is determined by the pole in the fermion Nambu-Gor'kov propagator. From the inverse propagator $S^{-1}(p_0, \mathbf{p}) \approx G^{-1}(p_0, \mathbf{p})$ at leading order, we get:

$$\det[G^{-1}(p_0, \mathbf{p})] = 0, \quad (18)$$

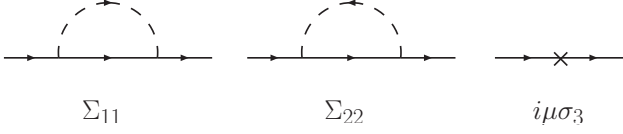


FIG. 4: Wavefunction renormalization. Same notation as in Fig. 1.

which gives $p_0 = \sqrt{\omega_p^2 + \chi_0^2} - \delta\mu$. At leading order in the ε -expansion, the quasiparticle energy has a minimum at $|\mathbf{p}| = 0$ with a gap $\Delta = \chi_0 - \delta\mu = 2\mu/\varepsilon - \delta\mu$:

$$p_0 = \chi_0 - \delta\mu + \frac{\omega_p^2}{2\chi_0}. \quad (19)$$

The gap decreases linearly with the asymmetry $\delta\mu$ and vanishes at the critical value $\delta\mu_c = 2\mu/\varepsilon$, where the gapless modes are the ones associated with the normal phase.

At next-to-leading order, the fermion propagator $S(p_0, \mathbf{p})$ gets a contribution from the self energy diagrams shown in Fig. 4. The condition for finding the pole in the fermion propagator $\det[S^{-1}(p_0, \mathbf{p})] = 0$ now reads:

$$\det[G^{-1}(p_0, \mathbf{p}) - \Sigma(p_0, \mathbf{p}) + i\mu\sigma_3] = 0. \quad (20)$$

The self-energy contribution $\Sigma(p_0, \mathbf{p})$ is diagonal in the Nambu-Gor'kov space and we find [5]:

$$\Sigma_{11}(p) = -g^2 \int \frac{d^{d+1}q}{(2\pi)^{d+1}} G_{22}(q) D(p-q), \quad (21)$$

$$\Sigma_{22}(p) = -g^2 \int \frac{d^{d+1}q}{(2\pi)^{d+1}} G_{11}(q) D(q-p).$$

Close to the minimum of the dispersion relation, we only need to use the leading order values $p_0 = \chi_0 - \delta\mu$, $\omega_p = 0$ to evaluate $\Sigma(p_0, \mathbf{p})$ [5]. We write $\Sigma(p_0, \mathbf{p}) \approx \Sigma^{(0)}(\chi_0 - \delta\mu, \mathbf{0}) + \Sigma^{(1)}(\chi_0 - \delta\mu, \mathbf{0})\omega_p/\chi_0$. Solving Eq. (20) gives

$$p_0 = \Delta + \frac{(\omega_p - \omega_0)^2}{2\chi_0}, \quad (22)$$

$$\Delta = \chi_0 - \delta\mu + i \frac{\Sigma_{11}^{(0)} + \Sigma_{22}^{(0)}}{2},$$

$$\omega_0 = \mu + i \frac{\Sigma_{22}^{(0)} - \Sigma_{11}^{(0)} - \Sigma_{11}^{(1)} - \Sigma_{22}^{(1)}}{2}.$$

The contribution from $\Sigma(p_0, \mathbf{p})$ to the dispersion relation at $\delta\mu = 0$ has been calculated before [5]. The $\delta\mu$ dependence comes from momentum q integrals that involve factors of $\Theta(\delta\mu - \sqrt{\omega_q^2 + \chi_0^2})$. Previously in Eq. (16) we found that $\delta\mu_c \approx \chi_0$. Thus for $\delta\mu \leq \delta\mu_c$, where the superfluid phase is thermodynamically stable, $\Sigma(p_0, \mathbf{p})$ is actually $\delta\mu$ independent. Therefore, we get

$$\Delta = \frac{2\mu}{\varepsilon} [1 + (3\hat{C} - 1 - 8\log 3 + 13\log 2)\varepsilon] - \delta\mu \quad (23)$$

$$\approx \frac{2\mu}{\varepsilon} [1 - 0.345\varepsilon] - \delta\mu,$$

$$\omega_0 = 2\mu.$$

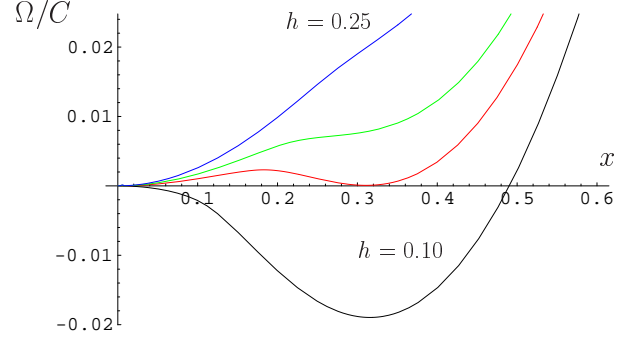
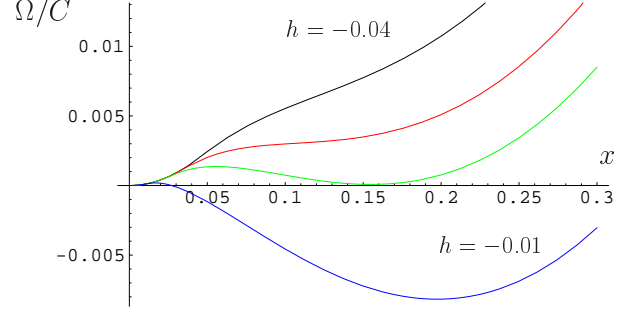


FIG. 5: Thermodynamic potential as a function of the supercurrent near the upper and lower critical chemical potential. We plot Ω/C as a function of x for different values of h . The scaling variables x, h are defined in the text. The upper panel shows $h = (-0.04, -0.03, -0.023, -0.01)$ and the lower panel shows $h = (0.10, 0.172, 0.20, 0.25)$.

We notice that Δ decreases linearly with $\delta\mu$ even at next-to-leading order. At the critical $\delta\mu_c$, the gap is

$$\Delta_c = \mu \frac{6\hat{C} + 2 - 48\log 3 + 73\log 2}{3} \approx 0.244\mu, \quad (24)$$

where we have set $\varepsilon = 1$. Thus, at this order of the calculation there are no gapless superfluid modes for $\delta\mu \leq \delta\mu_c$.

IV. STABILITY OF THE HOMOGENEOUS PHASE

We observed that there are no gapless fermion modes at $\delta\mu_c$. Nevertheless, given the size of next-to-leading order corrections to $\delta\mu_c$ and Δ the presence of gapless or almost gapless fermions can certainly not be excluded. Moreover, gapless modes might exist near the unitarity limit at finite scattering lengths. Gapless fermion modes in BCS-type superfluids cause instabilities of the homogeneous superfluid phase, see [19, 20, 21, 22, 23, 24]. The dispersion relation Eq. (22) is BCS-like, and we therefore investigate the stability of the homogeneous phase with regard to the formation of a non-zero

Goldstone boson current $\vec{v}_s = \vec{\nabla}\phi/m$. We note that the dispersion relation is only weakly BCS-like, $\omega_0 = O(\epsilon)$ whereas $\chi_0 = O(1)$. As a result any current that is formed is small, and we can neglect terms of higher order in v_s , or inhomogeneities in the absolute magnitude of χ_0 . The effective potential for v_s is

$$V_0(v_s) = \frac{1}{2}\rho v_s^2 + \int \frac{d^d p}{(2\pi)^d} E_p \Theta(-E_p), \quad (25)$$

where $\rho = nm$ is the mass density and $E_p = \Delta - \vec{p} \cdot \vec{v}_s + (\omega_p - \omega_0)^2/(2\chi_0)$ is the dispersion relation in the presence of a non-zero current. At leading order it is sufficient to compute the integral Eq. (25) in $d=4$ dimensions. A rough analytical estimate can be obtained by approximating the measure of the angular integration $\int_{-1}^1 dy \sqrt{1-y^2} \approx \int_{-1}^1 dy$. Introducing the scaling variables

$$x = \frac{(30\pi^3)^2}{\sqrt{2}} \frac{\rho^2 \beta^{9/2}}{\alpha^{7/2}} v_s, \quad (26)$$

$$h = - (30\pi^3)^2 \frac{\rho^2 \beta^5}{\alpha^4} (\Delta_0 - \delta\mu),$$

with $\Delta_0 = \Delta(\delta\mu=0)$, $\alpha = \omega_0/(2m\chi_0)$ and $\beta = 1/(8\chi_0 m^2)$ we can write the effective potential as [21]

$$\Omega \equiv V_0(v_s) - V_0(0) = C [f_h(x) - f_h(0)], \quad (27)$$

$$C = \frac{1}{(30\pi^3)^4} \frac{\alpha^7}{\rho^3 \beta^9},$$

where

$$f_h(x) = x^2 - \frac{(h+x)^{5/2}\Theta(h+x) - (h-x)^{5/2}\Theta(h-x)}{x}. \quad (28)$$

The functional $f_h(x)$ has non-trivial minima in the range $h \in [-0.067, 0.502]$. This means that there is a range of values

for $H = -(\Delta_0 - \delta\mu)/\Delta_0$ in which the ground state support a non-zero supercurrent. The size of this window is parametrically small, $O(\epsilon^6)$, and so is the magnitude of the current, $v_s \sim \epsilon^{11/2}$. Using the leading order results for ρ and the fermion dispersion relation we get $H_{min} = -0.24$ and $H_{max} = 1.84$. Numerical results for the complete energy functional in $d=4$ are shown in Fig. 5. The result is qualitatively very similar to the approximate solution, but the supercurrent window shrinks by about a factor 3. We get $H_{min} = -0.08$ and $H_{max} = 0.63$.

V. CONCLUSIONS

We used an expansion around $d = 4 - \epsilon$ spatial dimension to study the phase structure of a cold polarized Fermi gas at infinite scattering length. At next-to-leading order we find a single first order phase transition from a superfluid phase to a fully polarized normal Fermi liquid. The critical chemical potential is $\delta\mu_c = 1.06\mu$. We also find an unstable gapless Sarma phase. We observe that $O(\epsilon)$ corrections are sizable, and the presence of gapless superfluid phase cannot be excluded. We show that a gapless superfluid is unstable with respect to the formation of a supercurrent. Recent experiments [3] indicate the existence of a superfluid phase that carries net polarization. This suggests that the gapless phase is stabilized by finite temperature effects, finite size effects, or higher order corrections in the ϵ expansion.

Acknowledgments

This work was supported in parts by the US Department of Energy grants DE-FG02-03ER41260, DE-FG02-87ER40365 and by the National Science Foundation grant PHY-0244822.

-
- [1] M. W. Zwierlein, A. Schirotzek, C. H. Schunck and W. Ketterle, *Science* **311**, 492 (2006).
 - [2] G. B. Partridge, W. Li, Y. Kamar, R. I. and Liao and R. G. Hulet, *Science* **311**, 503 (2006).
 - [3] M. W. Zwierlein, A. Schirotzek, C. H. Schunck and W. Ketterle, *cond-mat/0605258*.
 - [4] Z. Nussinov and S. Nussinov, *cond-mat/0410597*.
 - [5] Y. Nishida and D. T. Son, *cond-mat/0604500*.
 - [6] J. Carlson, S.-Y. Chang, V. R. Pandharipande and K. E. Schmidt, *Phys. Rev. Lett.* **91**, 050401 (2003).
 - [7] S. Y. Chang, V. R. Pandharipande, J. Carlson and K. E. Schmidt, *Phys. Rev. A* **70**, 043602 (2004).
 - [8] G. E. Astrakharchik, J. Boronat, J. Casulleras and S. Giorgini, *Phys. Rev. Lett.* **93**, 200404 (2004).
 - [9] J. Carlson and S. Reddy, *Phys. Rev. Lett.* **95**, 060401 (2005).
 - [10] A. Bulgac, J. E. Drut and P. Magierski, *cond-mat/0505374*.
 - [11] E. Burovski, N. Prokof'ev, B. Svistunov and M. Troyer, *Phys. Rev. Lett.* **96**, 160402 (2006).
 - [12] D. Lee, *Phys. Rev.* **B73**, 115112 (2006).
 - [13] G. Sarma, *Phys. Chem. Solid* **24**, 1029 (1963).
 - [14] A. I. Larkin and Y. N. Ovchinnikov, *Zh. Eksp. Theor. Fiz.* **47**, 1136 (1964).
 - [15] P. Fulde and A. Ferrell, *Phys. Rev. A* **550**, 145 (1964).
 - [16] G. Rupak, *nucl-th/0605074*.
 - [17] W. V. Liu and F. Wilczek, *Phys. Rev. Lett.* **90**, 047002 (2003).
 - [18] P. F. Bedaque, H. Caldas and G. Rupak, *Phys. Rev. Lett.* **91**, 247002 (2003).
 - [19] S.-T. Wu and S. Yip, *Phys. Rev. A* **67**, 053603 (2003).
 - [20] M. Huang and I. A. Shovkovy, *Phys. Rev. D* **70**, 051501 (2004).
 - [21] D. T. Son and M. A. Stephanov, *Phys. Rev. A* **74**, 013614 (2006).
 - [22] T. Schafer, *Phys. Rev. Lett.* **96**, 012305 (2006).
 - [23] A. Kryjevski, *hep-ph/0508180*.
 - [24] A. Gerhold and T. Schäfer, *Phys. Rev. D* **73**, 125022 (2006).